TITLE: PFAS Porewater Concentrations in Unsaturated Soil: Field and Laboratory Comparisons Inform on PFAS Accumulation at Air-Water Interfaces

AUTHORS: Charles E. Schaefer[1,*], Dung Nguyen[2], Yida Fang[2], Nicholas Gonda[3], Chuhui Zhang[3], Stephanie Shea[3], Christopher P. Higgins[3]

AFFILIATIONS:

[1] CDM Smith, 110 Fieldcrest Avenue, #8, 6th Floor, Edison, NJ 08837 USA

[2] CDM Smith, 14432 SE Eastgate Way, # 100, Bellevue, WA 98007 USA

[3] Department of Civil and Environmental Engineering, Colorado School of Mines, Golden, CO 80401 USA

[*]**Address Correspondence to**: Charles E. Schaefer, CDM Smith, 110 Fieldcrest Avenue, #8, 6th Floor, Edison, NJ 088837. (732)-590-4633. E-mail: schaeferce@cdmsmith.com

Keywords

PFAS, AFFF, perfluorinated, lysimeter, porewater, soil

Abstract

Poly- and perfluoroalkyl substance (PFAS) leaching from unsaturated soils impacted with aqueous film-forming foams (AFFFs) is an environmental challenge that remains difficult to measure and predict. Complicating measurements and predictions of this process is a lack of understanding between the PFAS concentration measured in a collected environmental unsaturated soil sample, and the PFAS concentration measured in the corresponding porewater using field-deployed lysimeters. The applicability of bench-scale batch testing to assess this relationship also remains uncertain. In this study, field-deployed porous cup suction lysimeters were used to measure PFAS porewater concentrations in unsaturated soils at 5 AFFF-impacted sites. Field-measured PFAS porewater concentrations were compared to those measured in porewater extracted in the laboratory from collected unsaturated soil cores, and from PFAS concentrations measured in the laboratory using batch soil slurries. Results showed that, despite several years since the last AFFF release at most of the test sites, precursors were abundant in 3 out of the 5 sites. Comparison of field lysimeter results to laboratory testing suggested that the local equilibrium assumption was valid for at least 3 of the sites and conditions of this study. Surprisingly, PFAS accumulation at the air-water interface was orders of magnitude less than expected at two of the test sites, suggesting that PFAS accumulation at the air-water interface at AFFF-impacted sites may in some cases be less understood than anticipated. Finally, results herein suggest that bench-scale testing on unsaturated soils can in some cases be used to inform on PFAS in situ porewater concentrations.

1.0 Introduction

The leaching of poly- and perfluoroalkyl substances (PFAS) from unsaturated soils impacted with aqueous film-forming foam (AFFF) is an ongoing environmental challenge. While several bench-scale studies have evaluated PFAS leaching/desorption in either batch or column systems (Høisæter et al, 2019; McDonough et al., 2021; Schaefer et al., 2021; Rayner et al., 2022; Richardson et al., 2022; Bierbaum et al., 2023; Röhler et al., 2023), field-scale studies of PFAS leaching utilizing direct measures of unsaturated zone porewater with comparisons to bench-scale measurements are comparatively few in number. A small number of recent field studies have evaluated PFAS porewater concentrations and/or leaching from unsaturated soils historically impacted with AFFF (>20 years since the last AFFF application) (Quinnan et al., 2021; Schaefer et al., 2022; Anderson et al., 2022; Schaefer et al., 2023). These published field-scale studies have relied on the use of porous cup suction lysimeters and have typically been accompanied by collection and analysis of corresponding soil samples. Anderson et al. (2022) and Quinnan et al. (2021) reported on perfluoroalkyl acids (PFAAs) in porewater only. While Schaefer et al. (2022) evaluated both quantifiable and semi-quantifiable precursors (in addition to PFAAs) in porewater, precursor evaluation was hindered by either elevated quantification levels and/or variability in the data. Although porewater concentrations in the unsaturated zone were not directly measured, Ruyle et al. (2023) demonstrated that precursors accounted for approximately half of the PFAS-related organic fluorine at a site where over 20 years had elapsed since the last known AFFF release. Thus, the composition of the PFAS that are leaching from unsaturated soils at these historically-impacted sites remains poorly understood, particularly with respect to the presence of PFAA precursors.

When considering the ratio of PFAS soil concentrations to PFAS porewater concentrations measured in situ for historically AFFF-impacted unsaturated soils, Quinnan et al. (2021) observed ratios for PFOS that varied by a factor of 50 at a single site. Similarly, Anderson et al. (2022) observed ratios for several PFAAs that varied by up to an order of magnitude. Schaefer et al. (2023) observed ratios that increased by approximately a factor of 5 for PFOS during in situ flushing. While it has recently been argued that the relationship between measured PFAS soil concentrations and porewater concentrations in unsaturated soils can be impacted by complexities associated with adsorption at the air-water interface (Brusseau, 2018; Costanza et al., 2019; Schaefer et al., 2019; Silva et al., 2021), mass transfer (Brusseau et al., 2019; Schaefer et al., 2021), preferential flow (Zeng and Guo, 2023), and/or the presence of a slowly-desorbing fraction from the soil (Chen et al., 2016; Schaefer et al., 2022b), field data supporting such complexities remain sparse. Therefore, data relating in situ PFAS porewater concentrations to soil concentrations (via soil samples typically collected during site investigations) is needed for improved insights into leaching processes.

This study examined PFAS porewater concentrations measured at five AFFF-impacted sites, along with corresponding PFAS soil concentrations collected from the same depth interval as the porewater samples. In addition to evaluating the PFAS composition in the porewater, field-measured unsaturated zone porewater concentrations were compared to porewater concentrations measured in the laboratory via porewater extraction from collected soil cores, and also to dissolved PFAS concentrations measured in bench-scale saturated batch slurry experiments. Comparisons of these testing approaches provide insight into PFAS phase distribution and leaching in unsaturated soils, highlight challenges

104 with developing appropriate leaching tests, and note the potential importance of PFAA
105 precursor leaching in AFFF-impacted unsaturated zone source areas.
106
107 **2.0 Methods**
108 *2.1 Test Locations*
109 The five US Department of Defense sites evaluated in this study (denoted as Sites A
110 through E) are described in the Site Details in the Supplemental Materials. All studied sites
111 were exposed to AFFF, and most of the sites were interrogated as part of this study at least
112 a decade after the last known AFFF release. Soil properties, lysimeter installation depths,
113 porewater ionic strength, and average rainfall information are summarized for each test
114 location in Exhibit S1. Grain size distribution for each soil is provided in Exhibits S2-A
115 through S2-E. A summary of the testing for each site is provided in Table 1.
116
117 *2.2 Field Soil and Porewater Collection*
118 A 5.4-cm soil core was collected at each site using a gas-powered core sampling kit
119 (AMS, Inc., American Falls, ID). PFAS in the collected soil core were analyzed every 0.1
120 to 0.2 m for a total depth (depending on the site) of up to 2.4 m. Soil samples were also
121 collected for total organic carbon (TOC), cation exchange capacity, and moisture content.
122 Three lysimeters were installed within a 0.8 m radius of the soil core for Sites A, B, C, and
123 D; the borehole used for soil sampling was used for one of the installed lysimeters. For Site
124 E, three lysimeters were initially installed to a depth of 1.7 m below ground surface, but
125 failed to produce any water. Two lysimeters were then re-installed adjacent to the initial
126 locations to depths of 0.76 m below ground surface.

127 Lysimeter installation and sampling were performed as described previously (Schaefer
128 et al., 2022). Porous cup suction lysimeters (4.8 cm diameter), with 3.8 cm long ceramic
129 heads and a 2 bar bubbling pressure, were purchased from Soil Moisture Equipment Corp.
130 (Goleta, CA). A silica flour (200 mesh) slurry was poured into the lysimeter boreholes so
131 that the slurry reached several centimeters above the porous cup; addition of this slurry was
132 intended to maintain a saturated connection between the lysimeter and the native soil. A
133 sand was layered above the silica flour, with bentonite chips used to fill the remaining
134 annular space. A bromide tracer (500 mg/L bromide as NaBr) was included with the silica
135 flour slurry to account for any potential dilution of the porewater by the slurry water.
136 A hand pump was used to apply vacuum (typically 65 centibar) and extract porewater,
137 where several hours to overnight extraction was typically needed to collect water. When
138 possible, the initial sample of porewater collected for each lysimeter (approximately 20
139 mL) was used for purging and discarded; up to 3 subsequent rounds of porewater collected
140 for PFAS analysis were performed within a 2 to 6 day period. The first round of samples
141 from one of the 3 lysimeters at Site C was excluded from the dataset because PFAS
142 porewater concentrations were approximately two standard deviations less than that
143 observed in the other seven porewater samples collected. Exhibit S3 summarizes the
144 porewater samples collected from the lysimeters installed at each site.
145
146 *2.3 Bench-Scale Porewater Samples*
147 An additional intact soil core, collected during installation of the lysimeters, was
148 collected for bench-scale porewater testing. The purpose of the bench-scale porewater
149 testing was to serve as a comparison to the field-measured PFAS porewater concentrations,
150 where the bench-scale system represented a static (or, equilibrated) sample compared to

151 the dynamic (and potentially non-equilibrated) field sample. Bench-scale porewater
152 samples were collected using micro-sampling lysimeters that have a 0.95 cm outside
153 diameter, were 18 cm long, and have a porous ceramic head 3 cm in length (Soil Moisture
154 Equipment Corp., Goleta, CA). Vacuum (approximately 55 centibar) was applied to
155 collected soils using 10 mL disposable syringes, where the vacuum was typically applied
156 overnight. Methanol used to rinse the micro-sampling lysimeters and syringes was
157 collected and analyzed with the collected porewater to limit any PFAS sorptive losses to
158 the porewater extraction system; prior testing showed that sorptive losses to the field
159 lysimeters were negligible for PFOS (Schaefer et al. 2022). Ideally, porewater was
160 extracted from an intact core at the same depth where the field lysimeter was placed, with
161 2 additional duplicates extracted within 15 cm of this depth (3 samples total). However,
162 due to relatively dry soil conditions, only porewater from the Site D soil core could be
163 collected in this manner. For the other sites, soil was homogenized in the 20-30 cm depth
164 interval that overlapped the depth of the field lysimeter deployment; soil in this interval
165 was visually homogeneous. This soil was then wetted using a 5 mM $CaCl_2$ solution, packed
166 in polypropylene centrifuge tubes (approximately 80 g samples prepared in triplicate), and
167 equilibrated for a minimum of three days before extracting the porewater with the micro-
168 sampling lysimeters. Exhibit S4 shows the bench-scale porewater sampling set-up. Exhibit
169 S1 shows the soil moisture contents before and after wetting, where appropriate. Even after
170 wetting, porewater could not be extracted in the laboratory from the homogenized soil for
171 Site E, thus no bench-scale porewater samples were collected from Site E soil.
172
173 *2.4 Batch Soil Slurry Desorption Testing*

174 Using soil collected over the depth interval of the field-lysimeter porewater sampling,
175 batch slurry desorption tests were performed for Sites A, B, and C under saturated
176 conditions to further assess PFAS desorption equilibrium and interrogate the impacts of
177 air-water interfacial area collapse on PFAS release. Batch desorption testing was
178 performed using previously developed methodology (Schaefer et al., 2021). The soil
179 desorption reactors were prepared by mixing 30 g of soil with 100 mL of 5 mM $CaCl_2$
180 solution. Duplicate reactors were prepared for each soil. Aliquots of aqueous samples from
181 each reactor were collected over a 14- to 56-day period for target PFAS analysis
182 (quantifiable analytes) to ensure equilibrium was attained.
183
184 *2.5 Analytical*
185 Soil TOC was analyzed via combustion ion chromatography by Katahdin Analytical
186 Services, LLC (Scarborough, ME). Cation exchange capacity was analyzed by assessing
187 the exchangeable sodium cations by ALS Environmental (Houston, TX). PFAS soil
188 concentrations were analyzed via USEPA Draft Method 1633 by SGS AXYS Analytical
189 Services, Ltd (British Columbia, Canada). PFAS porewater concentrations were analyzed
190 by liquid chromatography high resolution mass spectrometry (LC-HRMS) for both
191 quantifiable (i.e., target) and semi-quantifiable (i.e., HRMS suspect) analytes at the
192 Colorado School of Mines using previously published methodologies (Hao et al., 2022;
193 Nickerson et al., 2020; Murray et al., 2019). Additional details of the PFAS porewater
194 analyses and reporting limits are provided in the Supplementary Materials (PFAS
195 Analytical). The acronyms and molecular formulas for the quantifiable and semi-
196 quantifiable PFAS identified in this study are also provided in the Supplemental Materials
197 (Exhibits S5 through S7).

198

199 *2.6 Estimation of air-water Interfacial Area*

200 To quantify the changes in the air-water interfacial area per unit volume ($a_{aw,}$) upon
201 wetting, the grain size distribution for each site soil was considered. The grain size
202 distributions for soils from the 5 sites are shown in Exhibit S2-A through S2-E. The
203 comparatively small grain size fractions associated with Sites C and E are readily apparent,
204 and are consistent with their clay contents shown in Exhibit S1. Assuming small pores
205 associated with small soil particles are wetted in the soil, the light (yellow) shading in
206 Exhibit S2-A through S2-E represent (approximately) the pore space wetted under field
207 conditions, while the dark (red) shading represents additional wetting in the homogenized
208 soil (from the collected soil core) used for the lysimeter micro-sampling.

209 For the three sites where the soils were wetted prior to the laboratory porewater
210 sampling (Sites A, B, and C) using the collected soil, the loss of air-water interfacial area
211 upon wetting can be estimated. The air-water interfacial area per volume of porous media
212 is estimated based on the correlation developed by Brusseau (2023):

213 $$a_{aw} = [-2.85S + 3.6]\,[3.9d^{-1.2}(1 - S)] \qquad \text{Eq. 1}$$

214 where d is the average particle diameter, S is the water saturation (volume water/volume
215 pore space), and a_{aw} is air-water interfacial area defined in units of cm^{-1}.

216 Using the grain size distributions shown in Exhibit S2-A through S2-E, and a soil bulk
217 density of 1.6 g cm^{-3} that is saturated at approximately 19% moisture content, the
218 parameters in Eq. 1 can be estimated under both the comparatively dry field conditions and
219 for the wetted conditions associated with the laboratory-collected (soil core) porewater
220 sampling.

221

3. Results and Discussion

3.1 PFAS Soil Concentrations

Quantifiable PFAS soil concentrations for each site are provided in Exhibit S8. It is noted that these results represent the sum of PFAS mass adsorbed to the soil, adsorbed at the air-water interface, and dissolved in the aqueous phase. Conventional environmental sampling refers to such measurements as soil concentrations, so this convention is retained herein. A more detailed mass balance assessment is provided in Section 3.3.

In all cases, PFOS exhibited the most elevated PFAS concentration measured in the collected soil samples. The perfluorinated sulfonate relative concentration versus depth profiles for Sites A and B show clear chromatographic separation (Fig. 1). The least hydrophobic compound (PFBS) has the deepest concentration maximum, while the PFOS concentration maximum is near the soil surface. In contrast, for Sites C and E, the relative concentration profiles are similar for each perfluorinated sulfonate, and no chromatographic separation was observed (Fig. 1). Site D is omitted from Fig. 1 due to the large number of perfluorinated sulfonate results that were below the analytical detection limit. Similar results with respect to the vertical concentration profiles were observed for the perfluorinated carboxylates (Exhibit S8). The reason for the differences between Sites A and B, and Sites C and E, are unclear, as they could be due to the nature of AFFF releases, rainfall, and/or other soil properties.

Semi-quantified PFAS in soil were analyzed at a single depth, corresponding to the approximate field lysimeter depth, for each site. Results are summarized in Exhibit S9. Estimated PFAS concentrations via semi-quantified analysis for suspect precursors should be interpreted with caution, as uncertainties remain as to the concentrations of compounds for which analytical standards are currently unavailable (Nickerson et al., 2020b; Pickard

et al., 2022). For the depths examined herein, quantified PFAS (predominantly PFOS) were the primary PFAS identified in the unsaturated soil samples. These findings are generally consistent with those obtained by Adamson et al. (2020), who showed that precursors only accounted for approximately 15% of the PFAS soil mass within the permeable sandy regions of the shallow saturated zone.

3.2 PFAS Porewater Composition using Field Lysimeters

PFAS porewater results for each site are summarized in Exhibit S10. A clear increasing trend in PFAS concentration with cumulative lysimeter sample volume was observed for some PFAS (i.e., increasing PFAS concentrations with increasing round number for a given lysimeter). This increasing trend was attributed to dilution of the porewater with slurry water added during lysimeter installation. The measured bromide concentration in the collected water from the lysimeters was used to calculate an appropriate dilution factor. Details of the dilution factor corrections are provided in the Supplemental Materials (Porewater Dilution Factors). Dilution factors greater than approximately two were only relevant for Sites A and B (Exhibit S10). The limited number of porewater samples (n=3) for Site B was due the difficulty in extracting porewater at this site; one lysimeter at Site B did not yield any porewater. Target (quantified) PFAS concentrations for each site, corrected for the appropriate dilution factor, are summarized in Fig. 2.

Sites B and E show that, despite more than a decade since the last known AFFF release, substantial (> 50 µg/L) levels of PFAS are migrating as either quantified (target) or suspect (semi-quantified) precursors in the porewater; again, semi-quantified analysis of suspect precursors should be interpreted with caution. Target precursors accounted for up to 70%

of the quantifiable PFAS fluorine mass for Site B. This observed persistence of precursors in the unsaturated zone porewater is consistent with previous studies that showed the persistence of precursors in shallow source area groundwater (Adamson et al., 2020; Ruyle et al., 2023). Overall, these results highlight the importance of improved understanding of precursor transformation in source areas to better evaluate the PFAS source function and mass discharge to groundwater. It is currently unclear as to why identified precursors were dominant in porewater for Sites B and E, but not for the other investigated sites; it is possible that the apparent lack of semi-quantified precursors at the other sites was due to lack of detection using the current analytical technique.

At Site A, porewater PFAAs were largely dominated by shorter-chained (≤6 perfluorinated carbons) compounds (Figure 2 and Exhibit S10). These porewater results are consistent with the corresponding soil data (Exhibits S8 and S9) collected at the lysimeter installation depth of 1.5 m below ground surface. For Site B, 4:2 FTS accounted for the majority of the identified PFAS mass in the porewater, although 4:2 FTS was only observed in one of the two water-producing lysimeters and was not observed in any soil samples. Besides this detection of 4:2 FTS, similar to Site A, porewater at Site B also was dominated by shorter-chained PFAS.

PFOS and/or PFHxS were the predominant PFAAs for Sites D and E. These results for Sites D and E are consistent with the soil data, and may reflect the greater migration of PFOS and PFHxS at these sites due to increased rainfall and shallower lysimeter placement compared to Sites A and B. In contrast to Sites D and E, the porewater data for Site C was not indicative of the soil concentrations, as PFPeA and PFHxA were the predominant porewater PFAAs despite the fact that PFOS was by far the predominant PFAA in the soil. This apparent discrepancy is likely due to the elevated affinity of PFOS to the soil

294 compared to PFPeA and PFHxA, and/or the relative affinity of PFOS to the air-water
295 interface (as discussed in Section 3.3). It is also possible the predominance of PFPeA and
296 PFHxA in Site C porewater was due to biotransformation of precursors present in Site C
297 soil.

298 Sulfonamides (FBSA, FHxSA, and/or PFOSA) were detected in porewater at all sites,
299 as were (with the exception of Site A) 4:2 FTS and/or 6:2 FTS. These PFAS are able to
300 biotically transform to PFAAs (Avendaño and Liu, 2015; Zhang et al., 2016; Ruyle et al.,
301 2023b). The presence of the sulfonamides in porewater, since they are not typically present
302 at high levels in AFFF formulations (Backe et al., 2013), suggests transformation of other
303 AFFF precursors to these sulfonamides has occurred or is occurring. Sites C and E, which
304 both had a substantial fraction of the PFAS-related fluorine in porewater associated with
305 FBSA, FHxSA, and/or PFOSA, showed elevated levels (compared to the other sites) of
306 MeFOSA, MeFOSAA, and AmPr-FHxSA in the soil; Site C also had Ampr-FPeSA and
307 AmPr-FOSA in the soil. The AmPr-sulfonamides have been shown to biotically transform
308 to perfluorinated sulfonamides and perfluorinated sulfonates (Cook et al., 2022), and thus
309 may serve as the source of these dissolved perfluorinated sulfonamides observed in the
310 porewater.

311 The semi-quantified suspect analytes identified in Site E porewater (Exhibit S10) were
312 dominated by the cationic sulfonamide-based compound TAmPr-N-MeFBSA, although
313 other zwitterionic sulfonamide-based suspect precursors (with 6 perfluorinated carbons)
314 also were present in the porewater. For Site C, a large number of suspect analytes were
315 identified in the porewater (Exhibit S10). The majority of the suspect precursors at Site C
316 were zwitterionic compounds with 6 or fewer perfluorinated compounds that were
317 identified in ESI+ mode. The two most abundant suspect analytes for Site C, SPrAmPr-

318 FHxSA and SPrAmPr-FHxSAA, are sulfonamide-based compounds. Barzen-Hanson et al.
319 (2017) reported that TAmPr-N-MeFBSA and SPrAmPr-FHxSA were present in 3M AFFF
320 formulations, so the findings herein indicate persistence of these released precursors at this
321 AFFF-impacted site.

322 Many of the precursors in the porewater samples measured for the study described
323 herein have been noted in previous investigations, but hitherto not directly measured via in
324 situ porewater sampling in the unsaturated zone. The presence of FHxSA and 6:2 FTS were
325 sporadically (likely due to detection limit issues) identified in a previous field porewater
326 study at an AFFF-impacted site (Schaefer et al., 2022). Nickerson et al. (2020), Ruyle et al
327 (2023), and the multi-site study of Adamson et al. (2022) also identified these precursors
328 in shallow groundwater at AFFF-impacted sites. With respect to the semi-quantified
329 precursors observed herein, Adamson et al. (2022) and Ruyle et al. (2023) identified
330 several sulfonamide-based precursors in shallow groundwater.

331

332

333 *3.3 Bench-Scale Porewater Samples*

334 A comparison of the quantified PFAS porewater concentrations measured in the field
335 lysimeters to those measured in the laboratory from the collected soil cores for each site,
336 with the exception of Site E (field data only), is provided in Figure 2. As noted in Exhibit
337 S1, the small soil grain size for Site E precluded extraction of porewater in the laboratory
338 from the collected soil core at the bench-scale. For Sites A and B, PFAS concentrations
339 measured in the field-collected porewater and in laboratory-collected porewater are
340 typically within a factor of 2 to 5. Given the potential pore-scale variability among field-
341 collected porewater and collected soil samples, such order of magnitude agreement is

342 considered reasonable. Notable exceptions for Sites A and B are PFOA and 6:2 FTS. For
343 PFOA, the limit of quantification (LOQ) for the field-collected porewater sample was 0.57
344 μg/L, which is just over 4-times less than that PFOA concentration measured in the
345 laboratory-collected porewater. The large (3 orders of magnitude) discrepancy for 6:2 FTS
346 in Soil B is not readily explained, but may be due to the variability of 6:2 FTS measured
347 between lysimeters in the field (greater than 50 μg/L in one lysimeter, but below the LOQ
348 of 0.11 μg/L at the other lysimeter; Exhibit S10).

349 For Site C, comparison between the field-collected porewater and laboratory-collected
350 porewater are similar to that observed for Sites A and B. However, the concentrations for
351 the long-chained compounds PFOS and 8:2 FTS are nearly 100-times greater in the
352 laboratory-collected porewater sample than in the field-collected porewater sample. PFOS
353 and 8:2 FTS are the most surface-active PFAS evaluated in this comparison (Lyu et al.,
354 2018; Brusseau et al., 2019), and the wetting (Exhibit S1) needed for the laboratory-
355 collected porewater sample likely caused a substantial decrease in air-water interfacial area
356 and subsequent release of PFAS into the aqueous phase (Schaefer et al., 2000; Schaefer et
357 al., 2023).

358 Based on the data in Exhibits S1 and S2A-S2E, Table 2 summarizes the parameters
359 used in Eq. 1 and the calculated a_{aw} values for each site. The change in a_{aw} upon wetting
360 (based on the difference in moisture content before and after wetting listed in Exhibit S1)
361 for Sites A and B are 250 cm^{-1} and 491 cm^{-1}, respectively. For Site C, the change in a_{aw}
362 upon wetting is 688 cm^{-1}, which is reflective of the increased fraction of small pores and
363 increased wetting associated with this soil. For Site D, no wetting of the soil was needed
364 (intact cores was used), so there was no change in a_{aw} between the field and laboratory.

The impacts of these changes in a_{aw} on the measured PFAS concentrations in the field-collected and laboratory-collected porewater were evaluated via mass balance for the field, laboratory core, and soil slurry systems (PFAS Mass Balance Evaluation along with Exhibit S12 are presented in the Supplemental Materials). A key component of this model was determination of the PFAS interfacial sorption coefficient (K_i). Values for K_i (Exhibit S12) were estimated using quantitative structure-property relationships (QSPRs) developed by Stults et al. (2023), which (in addition to perfluorinated chain length and molar volume) accounts for both the PFAS porewater concentration and porewater ionic strength.

For Sites A and B, both the predicted and measured PFOS porewater concentrations in the wetted laboratory soil cores were approximately equal to those measured in the field (Table 3). Thus, the results observed in Figure 2 for even the most surface active PFAS examined in this study (PFOS) are in agreement with the mass balance model predictions. Interestingly, to satisfy the mass balance (described in the Supplemental Materials), the PFOS K_i values were 2 to 3 orders of magnitude less than the QSPR predicted values, suggesting that PFOS accumulation at the air-water interfaces at Sites A and B was substantially less than anticipated. These large discrepancies between the experimental and QSPR-predicted K_i values for Sites A and B cannot be explained based on the selection of the Freundlich- isotherm utilized in the QSPR model by Stults et al., as K_i values employing a Langmuir-based modeling approach are only up to approximately 10-times less than the Freundlich-based QSPR values estimated using the Stults et al. QSPR model (Stults et al., 2022, 2023). These low K_i values are 2 to 3 orders of magnitude below the predicted K_i values and greatly inconsistent with experimental data generated by several different bench-scale studies (as summarized in Stults et al., 2023). One potential explanation for

389 the seemingly low PFOS K_i values is competitive sorption at the air-water interface. Prior
390 studies have shown that competitive PFAS sorption at air-water interfaces can occur
391 (Abraham et al., 2022; Huang et al., 2022; Guo et al. 2023), but such competitive effects
392 typically occur at PFAS concentrations that are orders of magnitude greater than observed
393 at these two sites. However, given the potential for yet unidentified compounds (e.g.,
394 hydrocarbon surfactants associated with AFFF) within the porewater matrix along with the
395 relatively (compared to Site C) low PFOS porewater concentrations, competitive effects
396 cannot be ruled out.

397 Air-water interfacial sorption from non-PFAS organic carbon (including natural
398 organic carbon) also has been shown to inhibit PFOS accumulation at the air-water
399 interface (Schaefer et al., 2022c). To further examine the potential for such inhibition in
400 Site A and B porewaters, the previously described film technique (Schaefer et al., 2019)
401 was used for Sites A and B to measure total organic carbon (TOC) accumulation at the air-
402 water interface. This methodology is described in the Supplemental Materials. Results of
403 this testing showed that substantial TOC sorption occurred at the air-water interface, with
404 TOC interfacial adsorption coefficients ($K_{i,TOC}$) of 1.3 cm and 0.38 cm for Sites A and B,
405 respectively. With TOC concentrations of approximately 1 mg/L in the tested waters, the
406 TOC air-water interfacial mass exceeds that of the PFAS interfacial mass by several orders
407 of magnitude. Thus, it is plausible that TOC interfacial accumulation is inhibiting PFAS
408 accumulation at the air-water interface for Sites A and B.

409 In contrast, for Site C, PFOS and 8:2 FTS concentrations in the laboratory-measured
410 porewater (after wetting) is nearly 100-times greater than the field-measured porewater
411 concentrations (Table 3). The model-predicted PFOS values were reasonably
412 (approximately a factor of 4) close to the measured values in the laboratory-collected

413 porewater. Similarly, Table 2 shows that the predicted porewater concentrations for 8:2
414 FTS and PFHpS reasonably described (within a factor of approximately 2 to 3) the
415 increases in porewater concentrations observed upon wetting. As expected, the impact of
416 wetting on the porewater PFAS concentrations increased with increasing PFAS surface
417 activity (PFOS > 8:2 FTS > PFHpS). Of note, and discussed in the PFAS Mass Balance in
418 the Supplemental Materials, is that the PFOS K_i values at Site C (determined using the
419 QSPR model) were 2 to 3 orders of magnitude greater than those determined via mass
420 balance for Sites A and B; these elevated K_i values for Site C are largely responsible for
421 the observed impacts of wetting (and subsequent loss of air-water interfacial area) on PFOS
422 and 8:2 FTS porewater concentrations shown in Table 3 and Figure 2. For PFAS that are
423 less surface active than PFHpS (i.e., shorter-chained PFAS), the modeled increases in
424 porewater concentrations upon wetting were comparatively small (less than a factor of 2),
425 which is again generally consistent with the porewater data shown in Figure 2.
426 It is noted that the addition of the 5 mM $CaCl_2$ solution to the Site C porewater could
427 have resulted in up to a 50% dilution in the porewater ionic strength, though re-
428 equilibration of this added solution with the soil would likely have mitigated this dilution
429 effect. Cai et al. (2022), who examined soils with organic carbon levels similar to that
430 observed for Site C, showed that such small changes in ionic strength caused small (<50%)
431 increases in the K_d values for PFOS. Similarly, the modest changes in ionic strength in the
432 bench-scale experiments are expected to cause a minimal (~20%) change in adsorption to
433 the air-water interface (Stults et al., 2023). Thus, the differences observed between the
434 field- and bench-scale porewater concentrations in Table 3 are likely not due to changes in
435 porewater ionic strength.

Importantly, for Sites A, B, and C, the equilibrium mass balance model was consistent with the porewater data shown in Figure 2, assuming soil moisture and air-water interfacial area were considered. Thus, invoking a local equilibrium assumption for these sites under the conditions tested within this study is reasonable, and consistent with prior work (Schaefer et al., 2022). These results also confirm the ability, at least for the conditions of this study, of bench-scale soil testing to inform on PFAS porewater and leaching behavior in the field. However, it is noted that transient variability due to high precipitation events or other subsurface heterogeneities (e.g., preferential flow in well-structured soils) could invalidate this local equilibrium assumption.

For Site D, PFAS concentrations measured in the field-collected porewater were generally 5- to 100-times less than those measured in the laboratory-collected porewater; Site D soils were not wetted prior to the laboratory-scale sampling (intact core was used). Thus, unlike Sites A, B, and C, the local equilibrium assumption does not appear to be valid for Site D. The cause of this discrepancy was initially thought to be due to field conditions during lysimeter sampling, as rainstorms were occurring during sample collection that might have caused rapid infiltration and dilution of PFAS porewater concentrations. Sampling was repeated at this same Site D location several months later in absence of any rainfall (sampling included triplicate lysimeters and 3 rounds of porewater sample collection as before); PFAS porewater concentrations did not show any increasing/decreasing trend with sample round and PFAS porewater concentrations generally were within approximately a factor of two of those previously measured (data not shown). Thus, the orders of magnitude discrepancy between PFAS porewater concentrations measured in the field-collected and the laboratory-collected porewater could not be explained by rainfall and dilution effects.

460 While a conclusive explanation for the discrepancy between the field-collected and
461 laboratory-collected PFAS porewater concentrations for Site D is not resolved for this
462 study, it is noted that the backfilled material in Site D was quite heterogeneous. Specifically,
463 core logging noted what appeared to be polyethylene plastic sheeting and cm-sized pieces
464 of concrete/rubble intermittently dispersed within the soil cores. In addition, ground
465 penetrating radar (GPR) surveying performed prior to lysimeter installation showed several
466 anomalies throughout (Exhibit S13), indicating discontinuities throughout the interrogated
467 zone and suggesting the presence of voids or other debris. Such discontinuities could result
468 in preferential or non-uniform flow that could bias PFAS concentrations in the lysimeters.
469 The applicability of porous cup suction lysimeters in this type of media warrants further
470 study.
471
472 *3.4 Batch Slurry Desorption*
473 To further evaluate the role of air-water interfaces in soils for Sites A, B, and C, PFAS
474 desorption in the batch slurry systems were evaluated. Desorption kinetics are provided in
475 Exhibit S14. The absence of increasing PFAS concentrations over time suggests that any
476 precursor biotransformation to the compounds shown in Exhibit S14 is slow relative to the
477 timescale of the laboratory porewater and batch experiments performed herein. As a final
478 evaluation of the impacts of wetting and air-water interface collapse on PFAS porewater
479 concentrations, PFAS concentrations in the batch experiments were compared to those
480 measured in the field lysimeters for Sites A, B, and C (Fig. 3). For Sites A and B, PFAS
481 concentrations in the batch experiments are much less than those measured in the field-
482 collected porewater. This is due to PFAS desorption and dilution in the comparatively high
483 liquid:solid ratio of the batch slurries compared to the unsaturated field soils. However, for

484 Site C, long-chained PFAS (i.e., PFOS, 8:2 FTS, PFHpS, and PFOA) concentrations in the
485 batch slurry systems are greater than those in the unsaturated field-collected porewater.
486 This is due to the collapse of all air-water interfaces in soil from Site C, the elevated air-
487 water interfacial area under unsaturated field conditions, and elevated values of K_i (Table
488 2 and as discussed in Section 3.3). Results for the shorter-chained and less surface-active
489 PFAS in Site C soil do not show an increase in concentration in the batch slurries relative
490 to unsaturated field conditions, which is consistent with air-water interfacial collapse being
491 responsible for the observed concentration increases for the longer-chained PFAS. Results
492 observed in Fig. 3 are consistent with those observed in Figure 2 and Table 3. Thus, both
493 sets of bench-scale testing (microlysimeter sampling and batch slurry desorption) are
494 qualitatively consistent with each other, and inform on field behavior.
495
496 **4.0 Conclusions and Environmental Implications**
497 Results of this study highlight the contribution of precursors in unsaturated zone
498 leachate from historically impacted AFFF source areas. The presence of these precursors
499 necessitates improved understanding regarding the long-term mass discharge and potential
500 transformation of these compounds, and their impact on site conceptual models.
501 Furthermore, results herein highlight the potential importance of PFAS accumulation at
502 air-water interfaces in unsaturated soils, and how moisture content can impact these
503 concentrations. However, PFAS accumulation at air-water interfaces in AFFF-impacted
504 soils may, in some cases, be substantially less than expected, suggesting that further
505 research in these complex systems may be required to predict PFAS leaching behavior.
506 Careful examination of soil moisture and texture, similar to that performed herein, may
507 serve useful in future studies. Finally, for the sites and conditions examined herein, bench-

scale testing using collected soils were shown to inform on field-scale behavior with respect to PFAS porewater concentrations. The utility of bench-scale testing, particularly for Site C soils, is dependent upon proper accounting of PFAS uptake at air-water interfaces. Improper accounting of air-water interfacial effects in saturated batch slurry testing could result in an overprediction of PFAS leaching in situ. Further research is recommended to determine the extent to which the findings herein can be applied to more complex unsaturated zone conditions including unsaturated zones that are very dry and deep, vadose zones with complex stratigraphy, and during extreme infiltration events.

5.0 Acknowledgments

Support for this research was provided in part by the Environmental Security Technology Certification Program (ESTCP) under Project ER20-5088. Views, opinions, and/or findings contained in this report are those of the authors and should not be construed as an official Department of Defense position or decision unless so designated by other official documentation.

6.0 References

Abraham, J.E., Mumford, K.G., Patch, D.J. and Weber, K.P. Retention of PFOS and PFOA mixtures by trapped gas bubbles in porous media. *Environ. Sci. Technol*. **2022**, 56, 15489-15498.

Adamson, D.T., Kulkarni, P.R., Nickerson, A., Higgins, C.P., Field, J., Schwichtenberg, T., Newell, C. and Kornuc, J.J. Characterization of relevant site-specific PFAS fate and transport processes at multiple AFFF sites. *Environ. Advances* **2022**, 7, 100167.

532 Adamson, D.T., Nickerson, A., Kulkarni, P.R., Higgins, C.P., Popovic, J., Field, J.,
533 Rodowa, A., Newell, C., DeBlanc, P. and Kornuc, J.J. Mass-based, field-scale
534 demonstration of PFAS retention within AFFF-associated source areas. *Environ. Sci.*
535 *Technol*. **2020**, 54, 15768-15777.
536 Anderson, R.H., Field, J.B., Dieffenbach-Carle, H., Elsharnouby, O. and Krebs, R.K..
537 Assessment of PFAS in collocated soil and porewater samples at an AFFF-impacted
538 source zone: Field-scale validation of suction lysimeters. *Chemosphere* **2022**, 308,
539 136247.
540 Avendaño, S.M. and Liu, J. Production of PFOS from aerobic soil biotransformation of
541 two perfluoroalkyl sulfonamide derivatives. *Chemosphere*, **2015**, 119, 1084-1090.
542 Backe, W.J., Day, T.C. and Field, J.A. Zwitterionic, cationic, and anionic fluorinated
543 chemicals in aqueous film forming foam formulations and groundwater from US
544 military bases by nonaqueous large-volume injection HPLC-MS/MS. *Environ. Sci.*
545 *Technol*. **2013** *47*, 5226-5234.
546 Barzen-Hanson, K.A., Roberts, S.C., Choyke, S., Oetjen, K., McAlees, A., Riddell, N.,
547 McCrindle, R., Ferguson, P.L., Higgins, C.P. and Field, J.A., 2017. Discovery of 40
548 classes of per-and polyfluoroalkyl substances in historical aqueous film-forming
549 foams (AFFFs) and AFFF-impacted groundwater. *Environ. Sci. Technol*. **2017**, 51,
550 2047-2057.
551 Bierbaum, T., Klaas, N., Braun, J., Nürenberg, G., Lange, F.T. and Haslauer, C.
552 Immobilization of per-and polyfluoroalkyl substances (PFAS): Comparison of
553 leaching behavior by three different leaching tests. *Sci. Total Environ.* **2023**, 876,
554 162588.

555 Brusseau, M.L. Assessing the potential contributions of additional retention processes to
556 PFAS retardation in the subsurface. *Sci. Total Environ*. **2018**, 613, 176-185.
557 Brusseau, M.L.. Determining air-water interfacial areas for the retention and transport of
558 PFAS and other interfacially active solutes in unsaturated porous media. *Sci. Total*
559 *Environ*. **2023**, *884*, 163730.
560 Brusseau, M.L.; Khan, N.; Wang, Y.; Yan, N.; Van Glubt, S.; Carroll, K.C.. Nonideal
561 transport and extended elution tailing of PFOS in soil. *Environ. Sci. Technol*. **2019**,
562 53, 10654-10664.
563 Cai, W., Navarro, D.A., Du, J., Ying, G., Yang, B., McLaughlin, M.J. and Kookana, R.S.
564 Increasing ionic strength and valency of cations enhance sorption through
565 hydrophobic interactions of PFAS with soil surfaces. *Sci. Tot. Environ.*, **2022**, 817,
566 152975.
567 Chen, H.; Reinhard, M.; Nguyen, V.T.; Gin, K.Y.H. Reversible and irreversible sorption
568 of perfluorinated compounds (PFCs) by sediments of an urban reservoir.
569 *Chemosphere* **2016**, 144, 1747–1753.
570 Cook, E.K., Olivares, C.I., Antell, E.H., Yi, S., Nickerson, A., Choi, Y.J., Higgins, C.P.,
571 Sedlak, D.L. and Alvarez-Cohen, L. Biological and chemical transformation of the
572 six-carbon polyfluoroalkyl substance N-dimethyl ammonio propyl perfluorohexane
573 sulfonamide (AmPr-FHxSA). *Environ. Sci. Technol.* **2022**, 56, 15478-15488.
574 Costanza, J.; Arshadi, M.; Abriola, L.M.; Pennell, K.D. Accumulation of PFOA and
575 PFOS at the air–water interface. *Environ. Sci. Technol. Letters* **2019**, 6, 487-491.
576 Guo, B., Saleem, H. and Brusseau, M.L. Predicting Interfacial Tension and Adsorption at
577 Fluid–Fluid Interfaces for Mixtures of PFAS and/or Hydrocarbon Surfactants.
578 *Environ. Sci. Technol* **2023**, 21, 8044-8052.

579 Hao, S., Choi, Y.J., Deeb, R.A., Strathmann, T.J. and Higgins, C.P. Application of
580 hydrothermal alkaline treatment for destruction of per-and polyfluoroalkyl substances
581 in contaminated groundwater and soil. *Environ. Sci. Technol.* **2022**, 56, 6647-6657.
582 Høisæter, Å., Pfaff, A. and Breedveld, G.D.. Leaching and transport of PFAS from
583 aqueous film-forming foam (AFFF) in the unsaturated soil at a firefighting training
584 facility under cold climatic conditions. *J. Contam. Hydrol.* **2019**, *222*, 112-122.
585 Huang, D., Saleem, H., Guo, B. and Brusseau, M.L. The impact of multiple-component
586 PFAS solutions on fluid-fluid interfacial adsorption and transport of PFOS in
587 unsaturated porous media. *Sci. Total Environ.* **2022***,* 806, 150595.
588 Li, X., Li, J.H. and Zhang, L.M. Predicting bimodal soil–water characteristic curves and
589 permeability functions using physically based parameters. *Computers Geotech.* **2014**,
590 57, 85-96.
591 Lyu, Y., Brusseau, M.L., Chen, W., Yan, N., Fu, X. Lin, X. Adsorption of PFOA at the
592 air–water interface during transport in unsaturated porous media. *Environ. Sci.*
593 *Technol*. **2018**, 52, 7745-7753.
594 McDonough, J.T., Anderson, R.H., Lang, J.R., Liles, D., Matteson, K. and Olechiw, T.
595 Field-scale demonstration of PFAS leachability following in situ soil stabilization.
596 *ACS Omega*, **2021**. 7, 419-429.
597 Murray, C. C.; Vatankhah, H.; McDonough, C. A.; Nickerson, A.; Hedtke, T. T.; Cath, T.
598 Y.; Higgins, C. P.; Bellona, C. L. Removal of per- and polyfluoroalkyl substances
599 using super-fine powder activated carbon and ceramic membrane filtration. *J.*
600 *Hazard. Mater. 2019, 366*, 160−168.

Nickerson, A., Maizel, A.C., Kulkarni, P.R., Adamson, D.T., Kornuc, J.J. and Higgins, C.P. Enhanced extraction of AFFF-associated PFASs from source zone soils. *Environ. Sci. Technol*. **2020b**, 54, 4952-4962.

Nickerson, A., Rodowa, A.E., Adamson, D.T., Field, J.A., Kulkarni, P.R., Kornuc, J.J. and Higgins, C.P. Spatial trends of anionic, zwitterionic, and cationic PFASs at an AFFF-impacted site. *Environ. Sci. Technol*. **2020**, 55, 313-323.

Peng, S. and Brusseau, M.L. Impact of soil texture on air-water interfacial areas in unsaturated sandy porous media. *Water Resour. Res.* **2005**, 41.

Pickard, H.M., Ruyle, B.J., Thackray, C.P., Chovancova, A., Dassuncao, C., Becanova, J., Vojta, S., Lohmann, R. and Sunderland, E.M.. PFAS and precursor bioaccumulation in freshwater recreational fish: implications for fish advisories. *Environ. Sci. Technol*. **2022**, 56, 15573-15583.

Quinnan, J.; Rossi, M.; Curry, P.; Lupo, M.; Miller, M.; Korb, H.; Orth, C.; Hasbrouck, K. Application of PFAS-mobile lab to support adaptive characterization and flux-based conceptual site models at AFFF releases. *Remed. J*. **2021**, 1–20.

Rayner, J.L., Slee, D., Falvey, S., Kookana, R., Bekele, E., Stevenson, G., Lee, A. and Davis, G.B. Laboratory batch representation of PFAS leaching from aged field soils: Intercomparison across new and standard approaches. *Sci. Total Environ.* **2022***,* 838, 156562.

Richardson, M.J., Kabiri, S., Grimison, C., Bowles, K., Corish, S., Chapman, M. and McLaughlin, M.J. Per-and poly-fluoroalkyl substances in runoff and leaching from AFFF-contaminated soils: a rainfall simulation study. *Environ. Sci. Technol.* **2022**, 56, 16857-16865.

624 Röhler, K., Susset, B. and Grathwohl, P. Production of perfluoroalkyl acids (PFAAs)
625 from precursors in contaminated agricultural soils: Batch and leaching experiments.
626 *Sci. Total Environ*. **2023**, 902,166555.
627 Ruyle, B.J., Thackray, C.P., Butt, C.M., LeBlanc, D.R., Tokranov, A.K., Vecitis, C.D.
628 and Sunderland, E.M., 2023. Centurial Persistence of Forever Chemicals at Military
629 Fire Training Sites. *Environ. Sci. Technol.* **2023**, 57, 8096-8106.
630 Ruyle, B.J., Schultes, L., Akob, D.M., Harris, C.R., Lorah, M.M., Vojta, S., Becanova, J.,
631 McCann, S., Pickard, H.M., Pearson, A. and Lohmann, R.. Nitrifying
632 Microorganisms Linked to Biotransformation of Perfluoroalkyl Sulfonamido
633 Precursors from Legacy Aqueous Film-Forming Foams. *Environ. Sci. Technol.*
634 **2023b**, 57, 5592-5602.
635 Schaefer, C.E.; Culina, V.; Nguyen, D.; Field, J. Uptake of Poly-and perfluoroalkyl
636 substances at the air–water interface. *Environ. Sci. Technol*. **2019**, 53, 12442–12448.
637 Schaefer, C.E., DiCarlo, D.A. and Blunt, M.J. Experimental measurement of air-water
638 interfacial area during gravity drainage and secondary imbibition in porous media.
639 *Water Resour. Res.* **2000**, 36, 885-890.
640 Schaefer, C.E.; Lavorgna, G.M.; Lippincott, D.R.; Nguyen, D.; Christie, E.; Shea, S.;
641 O'Hare, S.; Lemes, M.C.; Higgins, C.P.; Field, J. A field study to assess the role of
642 air-water interfacial sorption on PFAS leaching in an AFFF source area. *J. Contam.*
643 *Hydrol*. **2022**, *248*, 104001.
644 Schaefer, C.E., Lavorgna, G.M., Lippincott, D.R., Nguyen, D., Schaum, A., Higgins, C.P.
645 and Field, J.. Leaching of perfluoroalkyl acids during unsaturated zone flushing at a
646 field site impacted with aqueous film forming foam. *Environ. Sci. Technol*. **2023**, 57,
647 1940-1948.

Schaefer, C.E., Lemes, M.C., Schwichtenberg, T. and Field, J.A. Enrichment of poly-and perfluoroalkyl substances (PFAS) in the surface microlayer and foam in synthetic and natural waters. *J. Haz. Mat.* **2022c**, 440, .129782.

Schaefer, C.E., Nguyen, D., Christie, E., Shea, S., Higgins, C.P. Field, J.A. Desorption of Poly-and Perfluoroalkyl Substances from Soil Historically Impacted with Aqueous Film-Forming Foam. *J. Environ. Engin.* **2021**, 147, 06020006.

Schaefer, C.E.; Nguyen, D.; Christie, E.; Shea, S.; Higgins, C.P.; Field, J. Desorption isotherms for poly-and perfluoroalkyl substances in soil collected from an aqueous film-forming foam source area. *J. Environ. Engineer*. **2022b**, 148, 04021074.

Silva, J.A.; Martin, W.A.; McCray, J.E. Air-water interfacial adsorption coefficients for PFAS when present as a multi-component mixture. *J. Contam. Hydrol*. **2021**, 236, 103731.

Stults, J.F., Choi, Y.J., Rockwell, C., Schaefer, C.E., Nguyen, D.D., Knappe, D.R., Illangasekare, T.H. and Higgins, C.P. Predicting Concentration-and Ionic-Strength-Dependent Air–Water Interfacial Partitioning Parameters of PFASs Using Quantitative Structure–Property Relationships (QSPRs). *Environmental Sci. Technol.* **2023**, 57, 5203-5215.

Stults, J.F., Choi, Y.J., Schaefer, C.E., Illangasekare, T.H. and Higgins, C.P., 2022. Estimation of transport parameters of perfluoroalkyl acids (PFAAs) in unsaturated porous media: critical experimental and modeling improvements. *Environmental Sci. Technol.,* **2022**, 56, 7963-7975.

Zeng, J. and Guo, B. Reduced accessible air–water interfacial area accelerates PFAS leaching in heterogeneous vadose zones. Geophys. Res. Letters **2023**, 50, 2022GL102655.

672 Zhang, S., Lu, X., Wang, N. and Buck, R.C. Biotransformation potential of 6: 2
673 fluorotelomer sulfonate (6: 2 FTSA) in aerobic and anaerobic sediment. *Chemosphere*
674 **2016**, 154, 224-230.
675
676

TABLES

Table 1. Summary of PFAS testing and evaluations performed for each Site.

Test or Evaluation	Site A	B	C	D	E
Field PFAS Soil Concentrations (Fig. 1 and Exhibits S8 and S9)	✓	✓	✓	✓	✓
Field PFAS Porewater Concentrations (Fig. 2 and Exhibit S10)[1]	✓	✓	✓	✓	✓
Laboratory PFAS Porewater Concentrations (Fig. 2)	✓	✓	✓	✓[2]	-[3]
Batch Desorption Testing (Exhibit S14)	✓	✓	✓	-	-
Detailed Mass Balance Evaluation[4]	✓	✓	✓	-	-

[1] Field porewater collection volumes and dilution factors are presented in the Supplemental Materials (Exhibits S3 and S11, respectively)

[2] No additional wetting of the core was needed, as was the case for Sites A, B, and C, thus the laboratory-based porewater from Site D was extracted from an intact core at field moisture

[3] Porewater could not be extracted from the bench-scale micro-sampling lysimeter

[4] Presented in the Supplemental Materials (p. 35-36), along with PFAS interfacial sorption coefficients (Exhibit S12 in the Supplemental Materials)

Table 2. Parameters used in Eq. 1 to determine a_{aw}. d is the average grain diameter and S is the water saturation. "Field" values refer to the in situ conditions, while "Lab" values refer to conditions after wetting for the bench-scale. soil core porewater extractions.

Site	d (cm)	S (Field)	S (Lab)	Field a_{aw} (cm^{-1})	Lab a_{aw} (cm^{-1})
A	0.030	0.18	0.37	675	425
B	0.0019	0.28	0.54	921	430
C	0.025	0.21	0.80	774	86
D*	0.067	0.68	0.68	279	279
E**	0.0050	0.67	-	1260	-

* intact core at field moisture was used for bench-scale testing, so "field" and "lab" parameters were identical

** porewater could not be extracted from the bench-scale lysimeter

Table 3 For Sites A, B, and C, comparisons of PFAS porewater concentrations measured in the field lysimeters (C_1) and in the wetted soil cores (C_2) to the model-predicted wetted soil core values. ± values indicate 95% confidence intervals. K_i values used for the model predicted porewater concentrations are provided in Exhibit S12. 8:2 FTS and PFHpS comparison for Sites A and B are not provided because these compounds were not detected in the porewater and/or in the soil (at the depth of the lysimeters) at these two sites.

	Measured Porewater Concentration In Situ (C_1) (µg/L)	Measured Porewater Concentration in Wetted Laboratory Cores (C_2) (µg/L)	Predicted Porewater Concentration (C_2) (µg/L)
Site A			
PFOS	6.2 ± 3.4	3.0 ± 0.37	6.6 ± 3.3
Site B			
PFOS	2.2 ± 2.0	0.78 ± 0.38	2.8 ± 2.0
Site C			
PFOS	13 ± 4.1	680 ± 460	164 ± 75
8:2 FTS	1.2 ± 0.46	52 ± 13	16 ± 6.0
PFHpS	0.36 ± 0.051	2.9 ± 2.0	5.9 ± 3.4

FIGURES

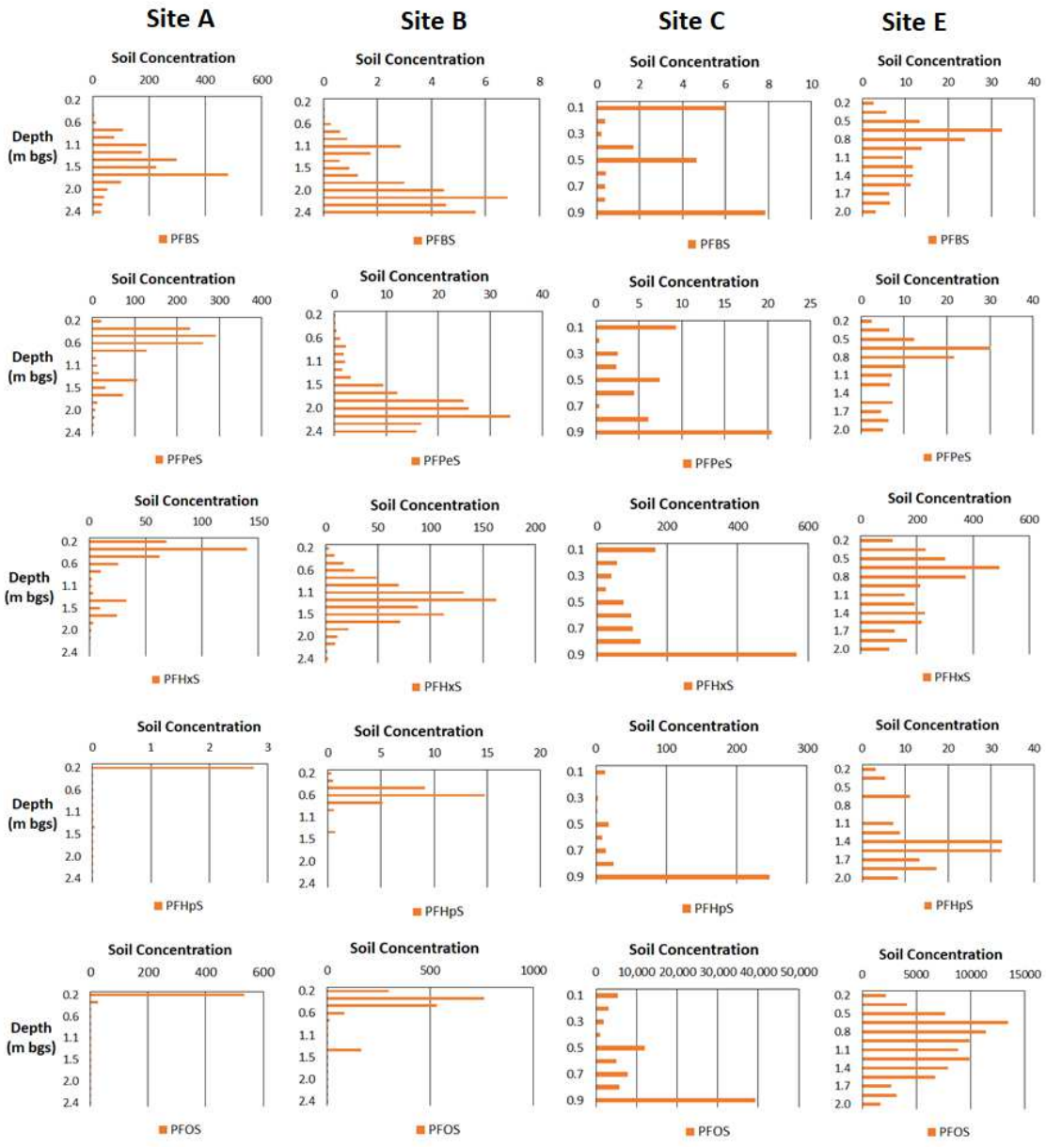

Figure 1. Perfluorinated sulfonate soil concentrations (µg/kg) measured as a function of depth in the unsaturated zone for sites A. B, C, and E. Non-detect results are plotted as 10% of the reporting limit. PFBS =perfluorobutanesulfonate, PFPeS=perfluoropentanesulfonate, PFHxS = perfluorohexanesulfonate, PFHpS= perfluoroheptanesulfonate, and PFOS = perfluorooctanesulfonate.

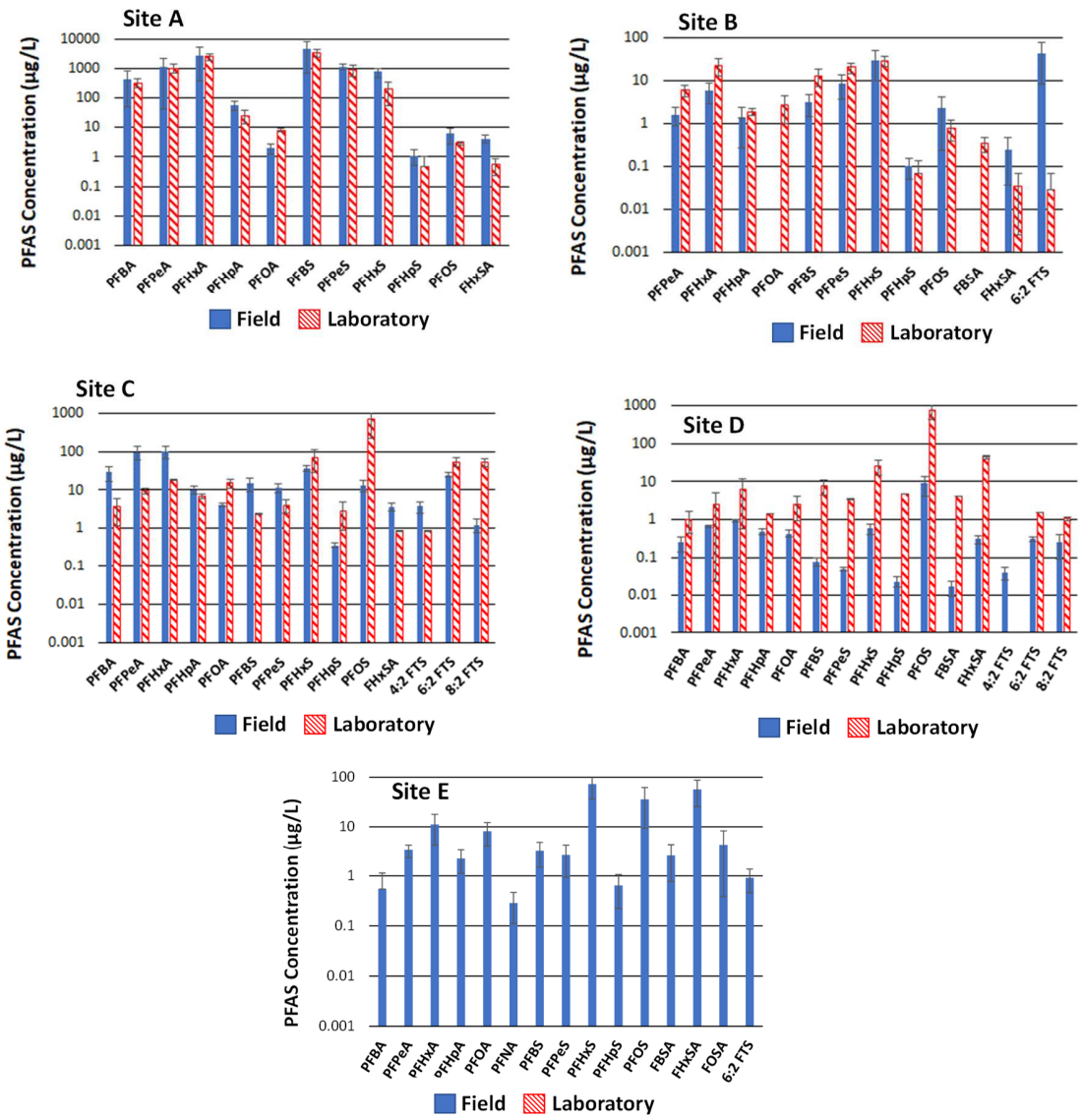

Figure 2. PFAS porewater concentrations for quantifiable analytes from both the field-deployed lysimeters and in the laboratory using porewater from the collected soil cores. Error bars represent 95% confidence intervals. For Site E, laboratory-based porewater samples could not be collected.

737
738

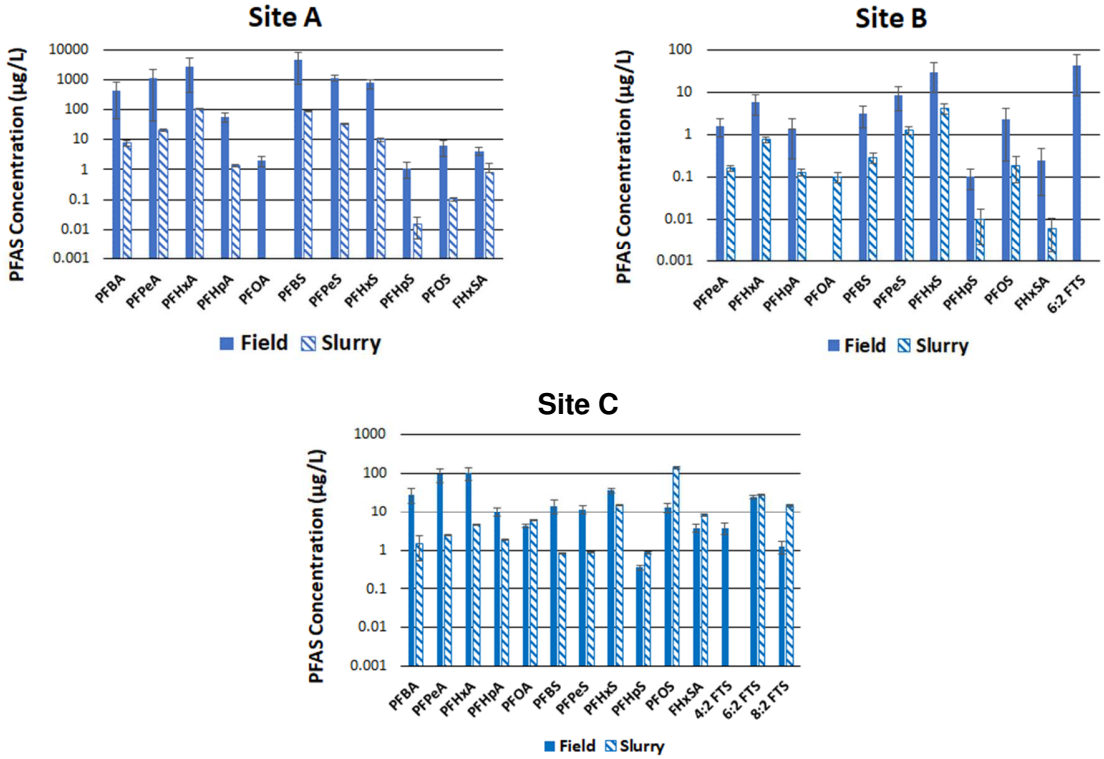

739
740 **Figure 3**. Comparisons between PFAS porewater concentrations measured in the field
741 lysimeters to those measured in the laboratory batch slurries for Sites A, B, and C. Error
742 bars indicate 95% confidence intervals.
743